JOURNAL OF MATERIALS SCIENCE 17 (1982) 2792–2800

Flux pinning by thin planar defects

WILSON E. YETTER, EDWARD J. KRAMER
Department of Materials Science and Engineering, and the Materials Science Center, Cornell University, Ithaca, New York 14853, USA

Planar defects, specifically grain boundaries, are now recognized as a major source of flux pinning in many materials, including the commercial A–15 superconductors. Unfortunately little theoretical attention has been devoted to the interaction between a planar pinning centre and the flux line lattice (FLL) of a type II superconductor. A Ginzburg–Landau perturbational approach is used here to calculate the pinning force per unit area exerted by a thin isolated planar defect upon the FLL. The pinning force is considered to arise from electron scattering at the defect plane, which creates a perturbation in the Ginzburg–Landau parameter, κ. The method of approach is of general applicability, however, and is easily adapted to other pinning mechanisms encompassed by the perturbational formalism. Second order terms in the FLL energy are retained, as well as all significant higher order terms in the Fourier transforms both of the superconducting electron density $|\psi|^2$, and of $|\psi|^4$. It is shown that a large error results, except at very high fields, if the above terms are ignored. The functional dependence of the elementary pinning force on temperature and field are shown to vary somewhat with the nature of the material and the pinning defect.

1. Introduction

Flux pinning at point defects, that is defects considerably smaller than the coherence length, ξ, has for some period of time been the subject of advanced theoretical analysis. The elementary pinning force of some pinning centres such as small voids [1–3] and dislocation loops [4, 5], for example, may now be calculated with some degree of confidence. However, relatively little attention has been paid to planar defects, pinning centres which are much thinner than ξ but which extend many flux line lattice (FLL) spacings in height and breadth. An important example of such a centre is the grain boundary; grain boundaries have attracted much recent attention because of a growing realization of their role as the primary pinning centres in the technologically important A–15 materials such as Nb_3Sn. Other examples include thin plate-like precipitates, dislocation cell walls, interphase boundaries, or artificially introduced thin metallic or insulating layers.

For the purposes of this article the source of flux pinning will be taken to be electron scattering off the pinning plane; such scattering will create a perturbation in the Ginzburg–Landau parameter, κ. However any mechanism which may be incorporated into the Ginzburg–Landau perturbational formalism may easily be included in the following treatment. The motivation for focusing on electron scattering is two-fold:

(a) Zerweck [6] has shown that the perturbation in κ near a planar scattering centre may be large and far ranging, and

(b) a strong case may be made [7] for considering electron scattering to be the major source of high-angle grain boundary pinning in most "dirty" materials.

Because a perturbational method is used, only a small variation in κ is allowed; this is not strictly the case for many real defects, such as grain boundaries. The local magnetic field and the superconducting wave function, ψ, are assumed to be insignificantly perturbed. In the present treatment a perfectly rigid FLL is assumed. Specifically, the FLL is not allowed to deform in the plane normal to the field direction or bend away from the field direction. Such a restriction is of course highly

0022–2461/82/102792–09$03.58/0

unrealistic; an undistorted flux lattice cannot even be pinned by randomly distributed pinning centres [1]!

The reader should bear in mind that the elementary pinning force per unit area of pinning plane, $\hat{f}_p$, is being calculated here and not the experimentally measured global pinning force F_p. F_p depends not only on $\hat{f}_p$, but also upon the process of force summation which occurs when the elastically interconnected lattice of fluxoids interacts with an array of pinning planes. The summation process is poorly understood, so direct comparison with experiment cannot be made except in a very few cases where measurements on single grain boundaries have been performed [8]. It is hoped that specimen preparation techniques will be found in the future to permit the study of flux pinning by single grain boundaries in a variety of materials, and with a variety of boundary structures. Once it is shown that planar pinning forces may be calculated with a reasonable degree of confidence an empirical pinning summation curve may be constructed, as has been done for point pinning [9].

Even in the case of multiple pinning planes, however, many properties of $\hat{f}_p$, such as the dependence of the pinning force on material, impurity level [7], the structure of the defect plane, or temperature, should be observable in a qualitative fashion, despite the summation problem. If nothing else, $\hat{f}_p$ should define the upper limit of F_p per unit area of pinning plane.

2. The calculation of the elementary pinning force

The defect-induced perturbation in FLL energy, $\delta E(\mathbf{r})$, may be written [1] in either the form

$$\delta E(\mathbf{r}) = \int_{\mathbf{r}'} \mu_0 H_c^2 \left\{ -\frac{\delta H_{c2}(\mathbf{r}')}{H_{c2}} |\psi(\mathbf{r}-\mathbf{r}')|^2 + \frac{1}{2}\frac{\delta\kappa^2(\mathbf{r}')}{\kappa^2} |\psi(\mathbf{r}-\mathbf{r}')|^4 \right\} d\mathbf{r}', \quad (1)$$

or

$$\delta E(\mathbf{r}) = \int_{\mathbf{r}'} \mu_0 H_c^2 \left\{ \left(-\frac{\delta H_c(\mathbf{r}')}{H_c} - \frac{\delta\kappa(\mathbf{r}')}{\kappa} \right) \times |\psi(\mathbf{r}-\mathbf{r}')|^2 + \frac{\delta\kappa(\mathbf{r}')}{\kappa} \times |\psi(\mathbf{r}-\mathbf{r}')|^4 \right\} d\mathbf{r}', \quad (2)$$

where $\mathbf{r}$ is the displacement of the FLL origin (chosen for convenience as the centre of a fluxoid) from the co-ordinate origin located on the pinning plane, μ_0 is the permeability of free space, H_c is the thermodynamic critical field and H_{c2} is the upper critical field; the integration is performed over all values of the position vector $\mathbf{r}'$. If we consider only the electron scattering component, Equation 2 reduces to

$$\frac{\delta E(\mathbf{r})}{\mu_0 H_c^2} = \int_{\mathbf{r}'} -\frac{\delta\kappa(\mathbf{r}')}{\kappa} |\psi(\mathbf{r}-\mathbf{r}')|^2 + \frac{\delta\kappa(\mathbf{r}')}{\kappa} \times |\psi(\mathbf{r}-\mathbf{r}')|^4 \, d\mathbf{r}'. \quad (3)$$

Direct evaluation of Equation 3 is quite awkward, but if the equation is cast in terms of the Fourier transforms of the order parameter and $\delta\kappa/\kappa$ it may be reduced to a simple form [10]. By invoking the convolution theorem in three dimensional space Equation 3 becomes

$$\frac{\delta E(\mathbf{r})}{\mu_0 H_c^2} = \int_{\mathbf{g}} \gamma_3(\mathbf{g})\{\Phi_2(\mathbf{g}) - \Phi_4(\mathbf{g})\} \exp(i\mathbf{g}\cdot\mathbf{r}) d\mathbf{g}. \quad (4)$$

Here the integral is over all reciprocal space; γ_3 is the three-dimensional Fourier transform of $(-\delta\kappa/\kappa)$, Φ_2 is the transform of $|\psi|^2$, and Φ_4 is the transform of $|\psi|^4$.

Let the lattice vectors, $\mathbf{g}_\nu$, of the reciprocal FLL be defined with the aid of Fig. 1. The basis vectors for the real space lattice are $\mathbf{a}$ and $\mathbf{b}$, chosen as shown, with magnitudes

$$|\mathbf{a}| = |\mathbf{b}| \equiv a_0 = (2\phi_0/(3)^{1/2}B)^{1/2}, \quad (5)$$

where a_0 is the fluxoid spacing, ϕ_0 is the magnetic flux quantum and B is the macroscopic magnetic flux density. If $\hat{z}$ is defined as a unit vector normal to the plane of Fig. 1, and so parallel to the applied field, then the reciprocal FLL basis vectors may be defined as:

$$\mathbf{g}_1 = 2\pi \frac{\mathbf{b}\times\hat{z}}{\mathbf{a}\cdot\mathbf{b}\times\hat{z}}, \quad |\mathbf{g}_1| = \frac{4\pi}{(3)^{1/2}a_0} \quad (6)$$

and

$$\mathbf{g}_2 = 2\pi \frac{\mathbf{a}\times\hat{z}}{\mathbf{a}\cdot\mathbf{b}\times\hat{z}}, \quad |\mathbf{g}_2| = |\mathbf{g}_1| \quad (7)$$

One may express $|\psi|^2$ and $|\psi|^4$ as cosine series summed over the $\mathbf{g}_\nu$ of the reciprocal FLL:

$$|\psi(\mathbf{r})|^2 = \sum_{\nu\neq 0} a_\nu (1 - \cos(\mathbf{g}_\nu\cdot\mathbf{r})), \quad (8)$$

$$|\psi(\mathbf{r})|^4 = \sum_{\nu=0} b_\nu \cos(\mathbf{g}_\nu\cdot\mathbf{r}). \quad (9)$$

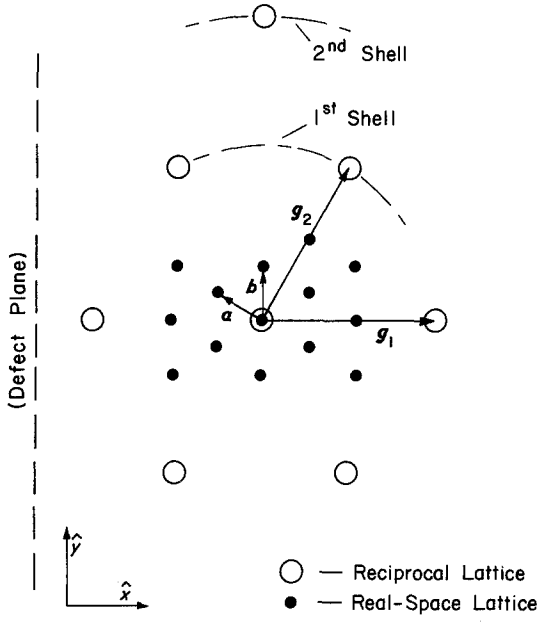

Figure 1 The real-space and reciprocal space flux line lattices, oriented so that $\mathbf{g}_1$ is normal to the defect plane, i.e. Orientation "1".

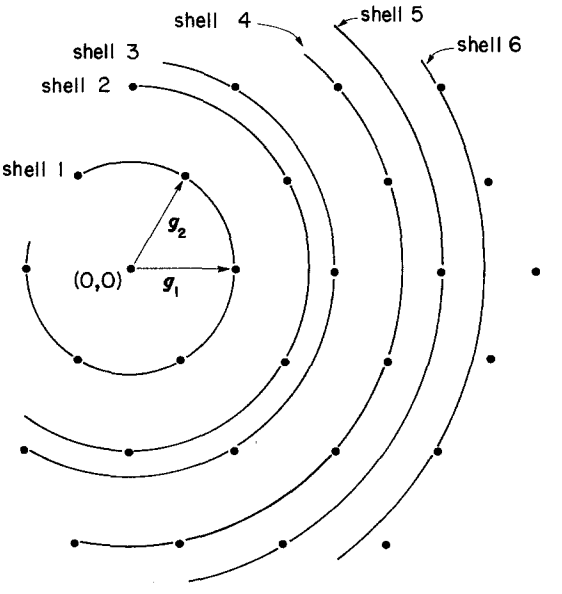

Figure 2 The reciprocal flux line lattice, showing the shell notation used to classify the reciprocal lattice vectors $\mathbf{g}_\nu$.

Note that in Equation 8 $\mathbf{g}_\nu = 0$ is excluded. The coefficients a_ν and b_ν are given in the Appendix. The a_ν have been calculated by Brandt [11] and the b_ν are derived in the Appendix. Both coefficients are functions of the reduced magnetic induction ($h = B/B_{c2}$, where $B_{c2} = \mu_0 H_{c2}$). It is convenient to define "shells" in the reciprocal FLL, each shell representing a set of reciprocal lattice points located at a common radius from the origin as shown in Fig. 2. Since all the a_ν and b_ν corresponding to $\mathbf{g}_\nu$ of equal magnitude are equal, the Fourier coefficients may be indexed by shell. For example, $a(n)$ equals the a_ν corresponding to any $\mathbf{g}_\nu$ vector in the nth shell.

The Fourier transforms (in three dimensions) of the various terms in Equations 8 and 9 are:

$$\mathcal{F}(\cos(\mathbf{g}_\nu \cdot \mathbf{r})) = (2\pi)^{3/2} \{\tfrac{1}{2}\delta(\mathbf{g}+\mathbf{g}_\nu) + \tfrac{1}{2}\delta(\mathbf{g}-\mathbf{g}_\nu)\}, \quad (10)$$

and

$$\mathcal{F}(1) = (2\pi)^{3/2}\,\delta(\mathbf{g}), \quad (11)$$

where δ is the Dirac delta function. Using Equations 8 to 11 one may write the Fourier transforms of $|\psi|^2$ and $|\psi|^4$ as

$$\Phi_2 \equiv \mathcal{F}(|\psi|^2) = (2\pi)^{3/2} \sum_{\nu \neq 0} a_\nu \{\delta(\mathbf{g}) - \tfrac{1}{2}\delta(\mathbf{g}+\mathbf{g}_\nu) - \tfrac{1}{2}\delta(\mathbf{g}-\mathbf{g}_\nu)\} \quad (12)$$

and

$$\Phi_4 \equiv \mathcal{F}(|\psi|^4) = (2\pi)^{3/2} \sum_{\nu=0} b_\nu \{\tfrac{1}{2}\delta(\mathbf{g}+\mathbf{g}_\nu) + \tfrac{1}{2}\delta(\mathbf{g}-\mathbf{g}_\nu)\}. \quad (13)$$

Equation 4 may now be written as

$$\frac{\delta E(\mathbf{r})}{\mu_0 H_c^2} = (2\pi)^{3/2} \int_{\mathbf{g}} \gamma_3(\mathbf{g}) \left[\sum_{\nu \neq 0} a_\nu \{\delta(\mathbf{g}) - \tfrac{1}{2}\delta(\mathbf{g}+\mathbf{g}_\nu) - \tfrac{1}{2}\delta(\mathbf{g}-\mathbf{g}_\nu)\} - \sum_{\nu=0} b_\nu \{\tfrac{1}{2}\delta(\mathbf{g}+\mathbf{g}_\nu) + \tfrac{1}{2}(\mathbf{g}-\mathbf{g}_\nu)\} \right] \exp(i\mathbf{g}\cdot\mathbf{r})\, d\mathbf{g}. \quad (14)$$

The development up to this point makes no assumptions about the geometry of the defect. Now, however, the planar nature of the pinning centre may be invoked to simplify Equation 14. The defect plane is defined as coincident with the plane $x = 0$ and of infinite extent in that plane. The perturbation in κ is constant over any plane parallel to the defect plane but falls off rapidly along the x-axis. Thus the transform of the perturbation will possess a rod-like form, such that γ_3 is non-zero only for $\mathbf{g}$ vectors located along a line in reciprocal space which passes through $\mathbf{g} = 0$ and is normal to the defect plane. This in turn means that non-zero terms may result in Equation 14 only (a) if the FLL is oriented such that the fluxoid line direction (i.e. the field direction) is parallel to the defect

plane, and (b) if at least one of the reciprocal lattice vectors $\mathbf{g}_\nu$ is normal to the plane. These conditions may be relaxed somewhat for a finite pinning plane (see Section 3.2).

For a very large pinning plane the above restrictions might at first seem to rule out the possibility of observing planar pinning experimentally. However since real pinning planes are imperfect, and since the FLL is not rigid but may bend and distort, a FLL which is slightly misoriented will interact weakly with the defect and will experience a torque tending to rotate it into alignment. Pinning defects in other parts of the specimen may place quite different orientational constraints on the FLL, in which case "grain boundaries" in the FLL, either pre-existing or newly formed, would allow local alignment. Such FLL grain boundaries have been observed [12] in a FLL pinned by crystal grain boundaries. It is reasonable to presume, with Evetts [13], that a continuous "recrystallization" of the FLL should occur during flux flow.

What if the FLL misorientation is not small and the FLL is pinned only weakly? Motion of the FLL will occur when the applied driving force $\mathbf{J} \times \mathbf{B}$ exceeds this weak pinning force. Because the FLL is composed of many "grains" rotated at various orientations around the field axis, new sections of the FLL will encounter the defect plane at (eventually) all possible orientations as they sweep through the plane. The FLL will become repinned when a "better" orientation arrives at the pinning plane. Thus the experimentally measured pinning force corresponds to the optimum possible orientation. For this reason only the orientation producing the largest δE need be considered. "Orientation 1", which is shown in Fig. 1, is the optimum pinning orientation for most materials and fields; in Orientation 1 $\mathbf{g}_1$ is normal to the pinning plane. "Orientation 2", rotated 30° with respect to Orientation 1, usually produces pinning larger near $h = 0.3$; in Orientation 2 $(\mathbf{g}_1 + \mathbf{g}_2)$ is normal to the defect plane.

Since the integral of Equation 14 vanishes except where $\mathbf{g}$ equals one of a set of $\mathbf{g}_\nu$ located along the x-axis, the integral may be reduced to a one-dimensional integral and the summation over ν may be limited to the shells which contain $\mathbf{g}_\nu$ vectors normal to the pinning plane. Using the shell notation, let $\mathbf{p}(n)$ represent the above set of $\mathbf{g}_\nu$ vectors. For Orientation 1 the relevant shells will be the set $n = n' = 1, 3, 5, 8\ldots$ and the $\mathbf{p}(n)$ will be integral multiples of $\mathbf{g}_1$. For Orientation 2 the relevant shells will be $n = n'' = 2, 6, 12\ldots$ and the $\mathbf{p}(n)$ will be integral multiples of $(\mathbf{g}_1 + \mathbf{g}_2)$.

Equation 14 for Orientations 1 or 2 therefore becomes

$$\frac{\delta E(\mathbf{r})}{\mu_0 H_c^2} = (2\pi)^{3/2}\Bigg[\Bigg\{\sum_{n',n''} a(n)\int_{\mathbf{g}\parallel\hat{\mathbf{x}}} \exp(i\mathbf{g}\cdot\mathbf{r})\,\gamma_3(\mathbf{g}) \times [\delta(\mathbf{g}) - \delta(\mathbf{g}+\mathbf{p}(n)) - \delta(\mathbf{g}-\mathbf{p}(n))]\,d\mathbf{g}\Bigg\} - b_0\int_{\mathbf{g}\parallel\hat{\mathbf{x}}} \gamma_3(\mathbf{g})\delta(\mathbf{g}) \times \exp(i\mathbf{g}\cdot\mathbf{r})\,d\mathbf{g} - \Bigg\{\sum_{n',n''} b(n)\int_{\mathbf{g}\parallel\hat{\mathbf{x}}} \exp(i\mathbf{g}\cdot\mathbf{r})\,\gamma_3(\mathbf{g}) \times [\delta(\mathbf{g}+\mathbf{p}(n)) + \delta(\mathbf{g}-\mathbf{p}(n))]\,d\mathbf{g}\Bigg\}\Bigg]. \quad (15)$$

In evaluating Equation 15 one should bear in mind (a) that there are two vectors i.e. $\pm\mathbf{p}(n)$ – contributing from each shell, (b) that γ_3 may be written here in terms of the one dimensional transform γ_1 since $\gamma_3 = (1/2\pi)\gamma_1$, and (c) that γ_1 is an even function. Equation 15 reduces to

$$\frac{\delta E(x)}{\mu_0 H_c^2} = (2\pi)^{1/2}\sum_{n',n''} a(n)\,\{\gamma_1(0) - 2\gamma_1(\mathbf{p}(n)) \times \cos(\mathbf{p}(n)x)\} - b_0\gamma_1(0) - 2b(n)\gamma_1(\mathbf{p}(n)) \times \cos(\mathbf{p}(n)x). \quad (16)$$

The position dependent pinning force per unit area is then

$$f_p(x) = -\frac{d}{dx}(\delta E) = -(2\pi)^{1/2}\,\mu_0 H_c^2 \times \sum_{n',n''} [a(n) + b(n)]\,2\mathbf{p}(n)\,\gamma_1(\mathbf{p}(n)) \times \sin(\mathbf{p}(n)x). \quad (17)$$

The FLL will shift position relative to the pinning plane in response to a driving force until at the critical current, J_c, the maximum pinning force is generated. Finding this position of maximum pinning analytically is not trivial however; although $a(n)$ and $b(n)$ decrease in magnitude as the shell index, n, rises, a number of shells must still be retained in the summation at all except the highest h. In practice the pinning force is calculated by computer, so the problem of maximization may be solved by scanning a range of values of $p(n)x$ from zero to 2π. Since Orientation 2 occasionally pro-

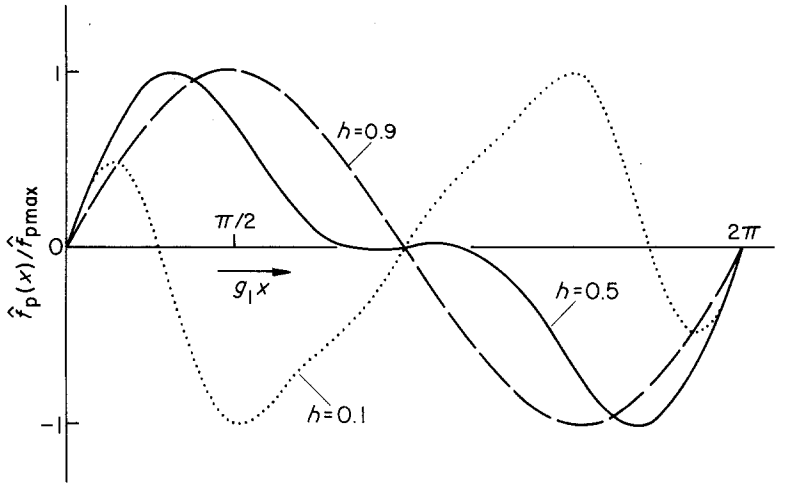

Figure 3 The normalized elementary pinning force, in Orientation 1, against g_1x. $g_1x = 0$ corresponds to a FLL row coincident with the defect plane; $g_1x = 2\pi$ is equivalent to one row spacing.

duces greater pinning, the maximum at both orientations must be compared to determine the overall maximum pinning force per unit area, $\hat{f}_p$.

The positional dependence of $\hat{f}_p$ (Orientation 1) for pinning at a grain boundary in Pb–18%Bi alloy is shown in Fig. 3. The general features of Fig. 3 are typical of flux pinning at a positive κ modulation. The interaction is repulsive at the fluxoid row positions. For high field (for example $h = 0.9$ in Fig. 3) the energy passes through a minimum half-way between the rows; $\hat{f}_p$ reaches a maximum when the nearest row is pushed to within one quarter row spacing of the defect plane. At lower fields the attractive contribution of the $|\psi|^4$ term in Equation 3 creates a double energy well and shifts the maximum in $\hat{f}_p$.

3. The high field approximation

3.1. The dependence on temperature and reduced field

Unless specific calculations are performed Equation (17) gives one little insight into the general behaviour of the pinning force. Certain approximations may be made in the regime of very high field, however which greatly simplify Equation 17. For $h > 0.9$ $a(1)$ is the only significant Fourier coefficient. Physically, this means that $|\psi|^2$ has a cosine-like form and that $|\psi|^4$, since it is proportional to $(1-h)^2$, is negligible at high h. The coefficient $a(1)$ approaches $(1-h)/6$ at high field [1], and since maximizing $f_p(x)$ now simply amounts to setting $|\mathbf{g}_1 x| = \pi/2$ the high field pinning approximation becomes

$$\hat{f}_p \simeq [(2\pi)^{1/2}/3]\,(1-h)\,\mu_0 H_c^2 g_1 \gamma_1(\mathbf{g}_1). \quad (18)$$

Recalling that $B = h\mu_0 H_{c2}$ and that $a_0^2 = (2\phi_0/(3)^{1/2})/B$, and defining $C_0 = (2\phi_0/(3)^{1/2})^{1/2}$, one may write $a_0 = C_0/(h\mu_0 H_{c2})^{1/2}$. Using this form of a_0 in the definition of $\mathbf{g}_1$, $\mathbf{g}_1 = 4\pi/(3)^{1/2}a_0$,

$$\hat{f}_p \simeq \left(\frac{32\pi^3}{27}\right)^{1/2} \cdot \frac{\mu_0^{3/2}}{C_0} \cdot H_c^2 H_{c2}^{1/2} h^{1/2}(1-h) \times \gamma_1\left(\frac{4\pi}{C_0(3)^{1/2}}\,[\mu_0 h H_{c2}]^{1/2}\right). \quad (19)$$

To emphasize the field and temperature dependence, non-relevant terms may be consolidated in the constants A and D, and the dependence on temperature (T) may be made explicit:

$$\hat{f}_p \simeq A H_c^2(T) H_{c2}^{1/2}(T) h^{1/2}(1-h)\gamma_1(D h^{1/2} H_{c2}^{1/2}(T)). \quad (20)$$

The $H_c^2 H_{c2}^{1/2}$ temperature dependence and the $h^{1/2}(1-h)$ field dependence are familiar from the literature. If γ_1 is a slowly varying function of $\mathbf{g}$ near $\mathbf{g}_1$, if for instance $\delta\kappa/\kappa$ is sharply peaked at $x = 0$ so that its transform is flat in reciprocal space, then the temperature dependence of γ_1 may be ignored. The function will have an important effect however if it varies rapidly near $\mathbf{g}_1$, for instance if the $\delta\kappa/\kappa$ function extends a distance of roughly $1/\mathbf{g}_1$ from the defect plane.

It is instructive to compare the results of the full-field and high field formulae for a specific example. Fig. 4 shows $\hat{f}_p$ against h for pinning by a grain boundary in Pb–16%Bi, using both Equations 17 and 19. Obviously the high field approximation is poor for most of the field range.

3.2. The effect of tilting the pinning plane

Pinning planes in real materials will of course be neither infinite in extent nor all aligned parallel

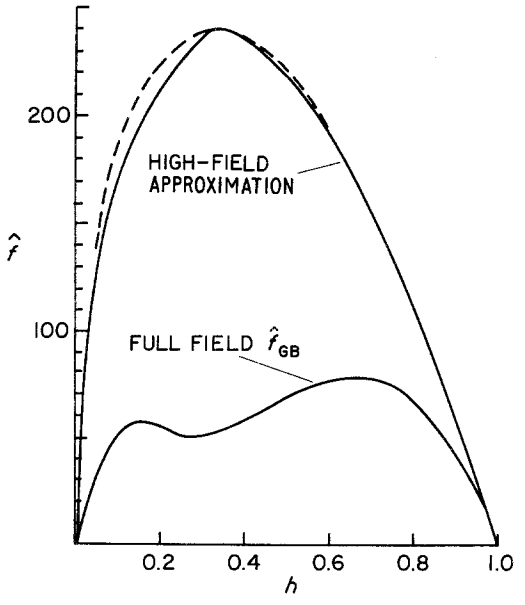

Figure 4 A comparison of $\hat{f}_p$ with the high-field approximation; the example is a grain boundary in Pb–16%Bi. The dashed line is $h^{1/2}(1-h)$, where $h = B/B_{c_2}$.

to the field direction. If tilting of the defect plane relative to the FLL is allowed, however, $\delta E(r)$ becomes very difficult to evaluate. Some limited insight nevertheless may be gained by making the high field assumptions of $b(n) = a(n > 1) = 0$ and $a(1) = (1-h)/6$. If θ is the tilt angle, then (for Orientation 1)

$$\frac{|\psi|^2}{1-h} = 1 - \frac{2}{3}\cos\left(\frac{2\pi y}{a_0}\right)\cos\left(\frac{[x\cos\theta - z\sin\theta]}{(3)^{1/2}} \times \frac{2\pi}{a_0}\right) - \frac{1}{3}\cos\left(\frac{2[x\cos\theta - z\sin\theta]}{(3)^{1/2}}\frac{2\pi}{a_0}\right). \quad (21)$$

If the defect plane is cut off sharply at height t and breadth a then

$$\gamma_3(\mathbf{g}) = \gamma_1(\mathbf{g}_x)\, D_a(\mathbf{g}_y)\, D_t(\mathbf{g}_z), \quad (22)$$

where

$$D_k(\mathbf{g}) = \frac{1}{(2\pi)^{1/2}}\frac{\sin(k\mathbf{g}/2)}{\mathbf{g}/2} \quad (23)$$

where k is either a or t. Having $|\psi|^2$ and γ_3 one may proceed as before to calculate $\hat{f}_p$. The result is complex, but may be approximated by

$$\hat{f}_p \simeq \left(\frac{a_0}{(6\pi)^{1/2}}\right)\mu_0 H_c^2 \mathbf{g}_1(1-h)\gamma_1(\mathbf{g}_1\cos\theta) \times \frac{1}{t\sin\theta}\sin\left(\frac{2\pi t\sin 6}{(3)^{1/2}a_0}\right) \quad (24)$$

The dependence on θ may be divided into two parts. $\gamma_1(\mathbf{g}_1\cos\theta)$ will be important only if γ_1 is rapidly varying near $\mathbf{g}_1$ or if θ is large. The second term, which is of the form

$$\frac{\sin(ct\sin\theta)}{t\sin\theta} \quad (25)$$

(with c a constant in θ) will severely limit the breadth of the $\hat{f}_p$ against θ profile unless t is very small. In most cases where multiple pinning planes exist in a specimen only a very small fraction can be simultaneously aligned with the applied field and therefore a narrow $\hat{f}_p$ against θ profile could severely limit the measured global pinning density F_p.

The measurements by Das Gupta *et al.* [8] of flux pinning by a single grain boundary in Nb seem to come close to the ideal case of pinning by a large, perfectly flat, pinning plane. The half-height width was found to be $\Delta\theta \simeq 1°$; t was 0.3 cm. Equation 24 however predicts a vanishingly small $\Delta\theta$. This discrepancy, and the fact that such an extreme requirement for alignment would make the experimental observation of planar pinning virtually impossible, leads us to conclude that considerable bending occurs in the FLL at small θ to locally bring the FLL parallel to the pinning plane. Such bending has of course not been allowed for in the model. Rudimentary calculations show that purely elastic bending is not sufficient. However many electron microscopy studies (using a decoration technique) have revealed a high density of defects in the FLL. Such defects might produce an effective "softening" of the FLL and allow much greater bending.

4. Conclusions

The component of the elementary flux pinning force due to electron scattering at a planar defect has been calculated in a manner valid for all $h > 0.1$, since (a) it includes the effect of the $|\psi|^4$ term in the Ginzburg–Landau perturbational expression and (b) it retains all significant Fourier components of $|\psi|^2$ and $|\psi|^4$. The model's most serious drawback is that it assumes a perfectly rigid FLL, which may neither distort in the plane normal to the applied field or bend away from the field direction. Other limitations include the requirement that $\delta\kappa/\kappa$ be small, which may weaken the validity of the calculation in some cases.

Pinning is found to be highly dependent on

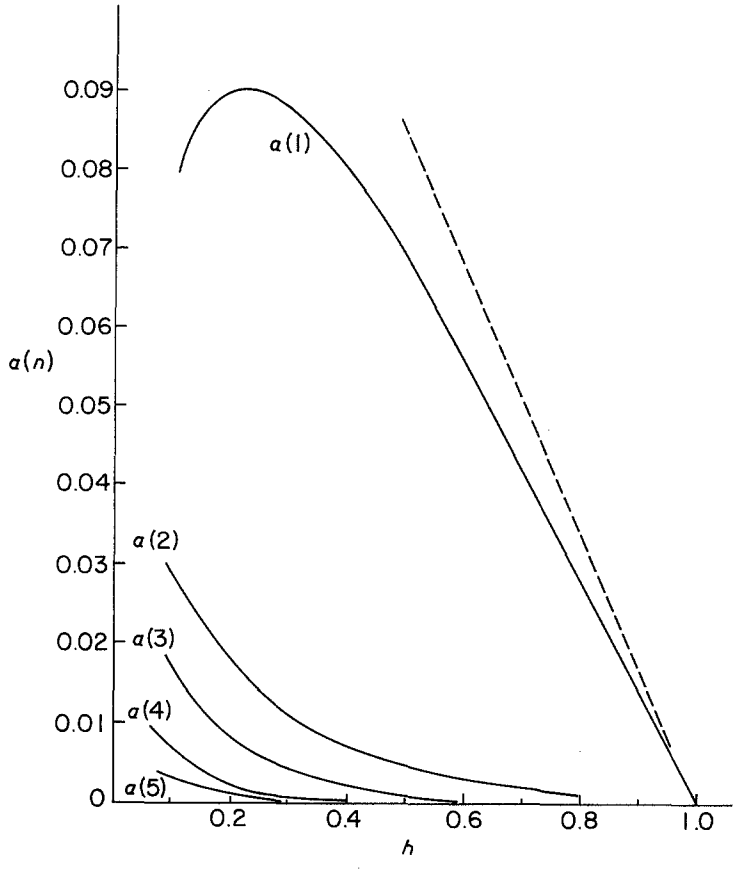

Figure A1 The Fourier coefficients $a(n)$ of $|\psi|^2$, as a function of reduced induction. The dashed line is $(1-h)/6$.

FLL/defect plane orientation, with the orientation shown in Fig. 1 producing the largest pinning for most fields and materials; a 30° rotation of the above orientation is sometimes more effective near $h = 0.3$. It is argued that an experimental measurement will always record the maximum pinning attainable by rotation of the FLL around the field axis. The interaction at $x = 0$, i.e. when the defect plane and FLL row are coincident, is repulsive; the maximum pinning force is exerted at a FLL defect spacing of roughly one quarter FLL row spacings. The high field approximation is shown to be seriously in error except for very high fields. At high field the dependence on h is approximately $h^{1/2}(1-h)$, and the temperatures dependence is largely contained in $H_c^2 H_{c2}^{1/2}$. At lower fields the h and T dependences cannot be expressed in closed form and vary somewhat with material.

Appendix: The Fourier coefficients of $|\psi|^2$ and $|\psi|^4$

In order to evaluate Equation 17 for the elementary pinning force the Fourier coefficients a_ν and b_ν (or in the shell notation $a(n)$ and $b(n)$) must be given numerical values. The $a(n)$ values have been published by Brandt [11] for the range $h > 0.1$. These $a(n)$ values are shown in Fig. A1.

The first step in finding the b_ν (or $b(n)$) values is to convert the cosine series for $|\psi|^2$ and $|\psi|^4$ into a complex Fourier series. From Equation 9,

$$|\psi|^4 = \sum_{\nu=0} b_\nu \left[\tfrac{1}{2} \exp(i\mathbf{g}_\nu \cdot \mathbf{r}) + \tfrac{1}{2} \exp(-i\mathbf{g}_\nu \cdot \mathbf{r})\right] \tag{A1}$$

For every $\mathbf{g}_\nu$ in the sum there is a $(-\mathbf{g}_\nu)$, so

$$|\psi|^4 = \sum_{\nu=0} b_\nu \exp(i\mathbf{g}_\nu \cdot \mathbf{r}). \tag{A2}$$

We can define C_j such that

$$|\psi|^2 = \sum_{j=0}^{j=\infty} C_j \exp(i\mathbf{g}_j \cdot \mathbf{r}) \tag{A3}$$

By comparing Equations 8 and A3 one may show that

$$C_0 = \sum_{\nu \neq 0} a_\nu \tag{A4}$$

and

$$C_j = -a_j \tag{A5}$$

The second step in finding the b_ν requires the con-

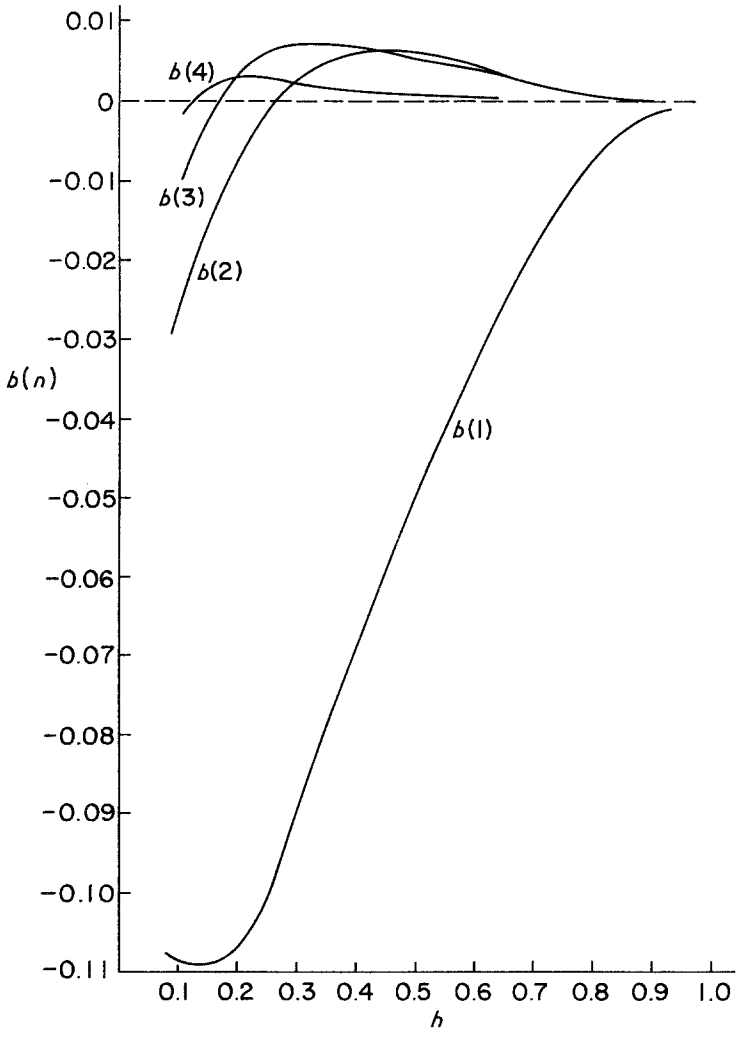

Figure A2 The Fourier coefficients $b(n)$ of $|\psi|^4$, as a function of reduced induction.

volution theorem in reciprocal space: let $t(\mathbf{r})$ and $s(\mathbf{r})$ be two functions in real space and let $\tilde{t}(\mathbf{g})$ and $\tilde{s}(\mathbf{g})$ be their Fourier transforms; then

$$\int \tilde{t}(\mathbf{g}')\,\tilde{s}(\mathbf{g}-\mathbf{g}')\,d\mathbf{g}' = \mathcal{F}[t(\mathbf{r})\cdot s(\mathbf{r})] \quad \text{(A6)}$$

where $\mathcal{F}$ is the Fourier transform operator. If $t = s = |\psi|^2$ then

$$\mathcal{F}(|\psi|^4) = \int \Phi_2(\mathbf{g}')\,\Phi_2(\mathbf{g}-\mathbf{g}')\,d\mathbf{g}'. \quad \text{(A7)}$$

But from Equation A2 it is clear that $\mathcal{F}(|\psi|^4)$ evaluated at some particular $\mathbf{g}_k$ is simply b_k, so

$$b_k = \int \Phi_2(\mathbf{g}')\,\Phi_2(\mathbf{g}_k-\mathbf{g}')\,d\mathbf{g}'. \quad \text{(A8)}$$

To evaluate the integral we may Fourier transform Equation A3, which gives

$$\Phi_2(\mathbf{g}') = \sum_{j=0} C_j(2\pi)^{-3/2} \int \exp(i\mathbf{g}_j\cdot\mathbf{r}) \times \exp(-i\mathbf{g}'\cdot\mathbf{r})\,d\mathbf{r} = \sum_{j=0} C_j\delta(\mathbf{g}'-\mathbf{g}_j). \quad \text{(A9)}$$

Similarly,

$$\Phi_2(\mathbf{g}_k-\mathbf{g}') = \sum_{j=0} C_j\delta(\mathbf{g}'-(\mathbf{g}_k-\mathbf{g}_j)). \quad \text{(A10)}$$

Substituting Equation A9 and A10 into Equation A8,

$$b_k = \int \sum_{j=0} C_j\delta(\mathbf{g}'-\mathbf{g}_j)\cdot\sum_{n=0} C_n\delta[\mathbf{g}'-(\mathbf{g}_k-\mathbf{g}_n)]\,d\mathbf{g}' \quad \text{(A11)}$$

The C_ν are determined by their associated reciprocal lattice vectors so for increased clarity one may use the notation $C(\mathbf{g}_\nu)$ instead. The integral of Equation A11 vanishes unless $\mathbf{g}_j = \mathbf{g}_k - \mathbf{g}_n$, so with some manipulation one finds that

$$b_k = \sum_{j=0} C(\mathbf{g}_j)\,C(\mathbf{g}_j+\mathbf{g}_k) \quad \text{(A12)}$$

This result (but without derivation or numerical evaluation) has been previously published by Brandt [14].

To help visualize the computation of b_k, imagine

two overlapping sets of reciprocal FLL points, shifted relative to each other by $\mathbf{g}_k$. A pair of C values is associated with each superimposed pair of lattice points. b_k is found by multiplying the C of one member of each pair of points times that of the other member, then summing all the products. The values of b_k (or alternately $b(n)$) are shown in Fig. A2.

Acknowldedgments

The authors wish to gratefully acknowledge the financial support of the U.S. Air Force Office of Scientific Research through grant number AFSOR–77–3107. This work also benefited from the use of the facilities of the Materials Science Center at Cornell, which is funded by the U.S. National Science Foundation.

References

1. A. M. CAMPBELL and J. E. EVETTS, *Adv. Phys.* **21** (1972) 199.
2. H. ULLMAIER, Springer Tracts in Modern Physics number 76 (Springer-Verlag, Heidelberg and New York, 1975) p. 1.
3. H. C. FREYHARDT, "Radiation-Induced Flux Pinning in Type II Superconductors" (Institut fur Metallphysik, Universität Göttingen, Germany, 1976) p. 1.
4. E. J. KRAMER, *Phil. Mag.* **33** (1976) 331.
5. C. S. PANDE, *Appl. Phys. Lett.* **28** (1976) 462.
6. G. ZERWECK, *J. Low Temp. Phys.* **42** (1981) 1.
7. W. E. YETTER, D. A. THOMAS and E. J. KRAMER, *Phil. Mag.* in press.
8. A. DAS GUPTA, C. C. KOCH, D. M. KROEGER and Y. T. CHOU, *Phil. Mag.* **B38** (1978) 367.
9. E. J. KRAMER, *J. Appl. Phys.* **49** (1978) 742.
10. E. J. KRAMER, *J. Electonic Mater.* **4** (1975) 839.
11. E. H. BRANDT, *Phys. Stat. Sol. (b)* **51** (1972) 345.
12. B. LISCHKE and W. RODEWALD, Proceedings of the International Discussion Meeting on Flux Pinning in Superconductors, Sonnenberg 1974, edited by P. Haasen and H. C. Freyhardt, Sonnenberg, September 1974 (Akademic der Wissenschaften, Göttingen, 1975) p. 322.
13. J. E. EVETTS, private communication.
14. E. H. BRANDT, *Phys. Stat. Sol. (b)* **84** (1977) 637.

Received 24 September 1981
and accepted 12 January 1982